Cadaveric study of deep temporal fascia for autologous rhinoplasty grafts: Dimensions of the temporal compartment in Asians

Daekwan Chi[1], Jae-Hee Kim[1], Taek-Kyun Kim[1], Jae Yong Jeong[1], Chungmin Shin[2], Sunje Kim[2], Sang-Ha Oh[2,3]

[1]The PLUS Plastic Surgery, Seoul; [2]Department of Plastic and Reconstructive Surgery, Chungnam National University Hospital, Daejeon; [3]Brain Research Institute, Chungnam National University College of Medicine, Daejeon, Korea

Background Due to the anatomical complexity of the deep temporal fascia (DTF), practical guidelines for its safe harvest are lacking. However, since the upper temporal compartment (UTC) contains no vital structures, it may provide safe access for DTF harvest. This study aimed to identify the anatomical structures of the temporal compartment in Asian cadavers and to measure their dimensions to enable safe DTF harvest.

Methods The anatomical structures surrounding the temporal compartment were identified in 27 hemifaces from 15 Korean cadavers. After dissection, digital images were acquired and craniometric landmarks were placed upon them to identify the boundaries of the temporal compartment. The horizontal and vertical lengths of the temporal compartment were measured and their surface areas were computationally assessed. Subsequently, differences in the results by sex were evaluated.

Results The five-layer anatomical structure of the UTC was clearly visualized. The UTC was bounded by the temporal septa superiorly and inferiorly, the innominate fascia laterally, and the DTF medially. No vital structures were present within the UTC. The vertical and horizontal lengths of the UTC were 6.41 ± 0.67 cm and 10.44 ± 0.83 cm, respectively, and the surface area of the UTC was 48.52 ± 5.65 cm^2. No statistically significant differences were observed in any dimensions between male and female patients.

Conclusions During rhinoplasty, DTF can be harvested as an autologous graft material from the UTC. An anatomical understanding of the UTC will aid in the safe and simple harvest of a sufficient amount of DTF.

Keywords Fascia / Rhinoplasty / Cadaver

Correspondence: Sunje Kim
Department of Plastic and Reconstructive Surgery, Chungnam National University Hospital, 282 Munhwa-ro, Jung-gu, Daejeon 35015, Korea
Tel: +82-42-280-7381
Fax: +82-42-280-7384
E-mail: ksj9243@gmail.com

Sang-Ha Oh
Department of Plastic and Reconstructive Surgery, Chungnam National University Hospital, 282 Munhwa-ro, Jung-gu, Daejeon 35015, Korea
Tel: +82-42-280-7387
Fax: +82-42-280-7384
E-mail: djplastic@cnu.ac.kr

INTRODUCTION

In rhinoplasty, the deep temporal fascia (DTF) is among the most important autologous graft materials used for various purposes. The DTF is generally utilized alone or as a fascia-wrapped cartilage graft in soft tissue reinforcement in reconstructive rhinoplasty [1,2] and for radix augmentation, correcting dorsal skin irregularities, and reinforcing the tip skin in aesthetic rhinoplasty [3-5]. Since the DTF is harvested from the same surgical field as rhinoplasty and features lower donor site morbidity rates, the DTF has advantages over other autologous tissues such as dermofat tissue [6], tensor fascia lata [7], and mastoid fascia [8]. However, it also has disadvantages, including handling difficulties, partial absorption, donor site alopecia, discomfort due to muscle damage, and possible hematoma [9]. Furthermore, rhinoplasty surgeons are often reluctant to access the temporal area to harvest the DTF owing to its anatomical complexity. The temporal compartment consists of upper and lower parts, the former of which contains no vital structures [10-12]. Therefore, we hypothesized that the upper temporal compartment (UTC) could provide a safe space for DTF harvest. Based on this concept, this study aimed to identify the anatomical structures of the UTC and to measure its dimensions.

METHODS

This study was approved by the Research Ethics Board of the Chungnam National University Hospital (IRB No. 2019-03-042). From March 2019 to March 2020, 27 hemifaces (15 right, 12 left) from 15 Korean cadavers (eight males, seven females; mean age, 65 years) were used to identify the anatomical structures surrounding the temporal compartment. Three hemifaces in which it was difficult to identify landmarks were excluded prior to the study. The nomenclature of the layers and ligamentous structures followed those of a previous report by O'Brien et al. [11]. Two plastic surgeons (JHK and SJK) performed all dissections. Digital images were taken to measure the dimensions of the temporal compartments after full exposure.

Dissection

After palpation of the superior temporal ridge, an inverted U-shaped skin incision was made from the lateral brow to the mastoid area and the dissection continued from the superior temporal ridge to the upper border of the zygomatic arch in a layer-by-layer fashion.

Landmark identification and lengths and surface areas of the temporal compartments

Considering the difficulty of directly measuring the surface area in cadavers, indirect photogrammetric measurements were performed. To obtain more objective measurements, we chose craniometric landmarks and semi-landmarks in the temporal area as described in previous studies (Table 1, Fig. 1) [13,14]. Two observers separately placed landmarks on each cadaver image and measured the dimensions of the temporal compartment using Digimizer version 3.1.2.0 software (MedCalc, Mariakerke, Belgium). The vertical and horizontal lengths of the entire temporal compartment (ETC) and the UTC were measured. Subsequently, the surface area of the ETC, UTC, and lower temporal compartment (LTC) were computationally assessed.

No.	Type	Landmarks[a]	Brief definition
1	Landmark	Stephanion	The point at which the inferior temporal line crosses the coronal suture
2	Landmark	Frontotemporale	The point located generally forward and inward on the superior temporal line directly above the zygomatic process of the frontal bone
3	Landmark	Marginal process lateral	The most posterior portion of marginal process, taken on the lateral surface of the zygomatic bone
4	Landmark	Jugale	The deepest point in the curvature of the frontal and temporal malar processes
5	Landmark	Radiculare	The point on the lateral aspect of the root of the zygomatic process at the deepest incurvature
6	Semi-landmark	Otobasion superius	The highest point of attachment of the external ear to the scalp
7	Semi-landmark	SM point	The most laterally positioned point on the supra-mastoid crest
8	Semi-landmark	P point	The posterior point of the temporal fossa or the superior temporal line perpendicular to the Frankfurt horizontal line
9	Semi-landmark	SP point	The point between the superior point of the superior temporal line and the posterior point of the superior temporal line
10	Semi-landmark	S point	The superior point of the temporal fossa or the superior temporal line at the Frankfurt horizontal line
11	Semi-landmark	ITSS point	The starting point of the inferior temporal septum on the temporal ridge
13-20	Semi-landmark	ITSE point	The end point of the inferior temporal septum on the upper border of the zygomatic arch

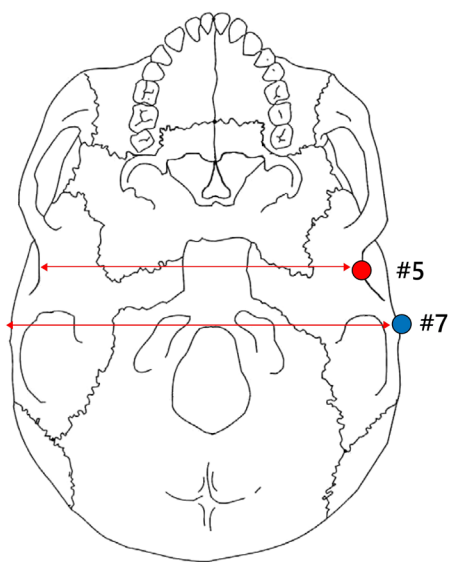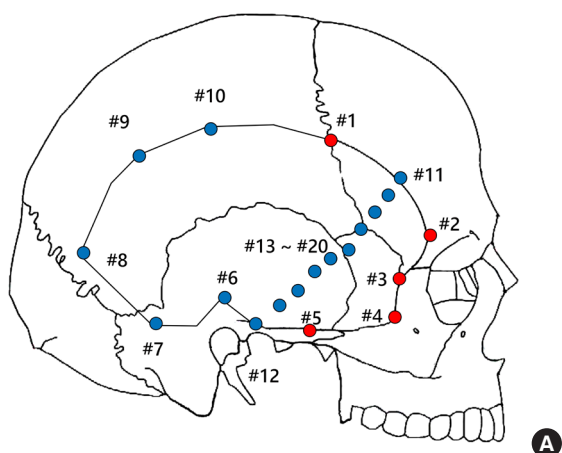**Table 1. Definition of craniometric landmarks and semi-landmarks**

[a]The landmarks chosen for this study were previously used by researchers such as Noback and Harvati [13] and Toro-Ibacache et al. [14] following standard definitions.

Chi D et al.   Deep temporal fascia in Asian cadavers

Archives of Plastic Surgery APS

Statistical methods

Statistical analysis was conducted using IBM SPSS Statistics for Windows version 27 (IBM Corp., Armonk, NY, USA). The average values of all the dimensions were analyzed. Data are presented as mean ± standard deviation. Subsequently, the independent t-test was performed to analyze differences between males and females. In addition, the intraclass correlation coefficient was used to evaluate intraobserver and interobserver reliability. Ten cadavers were chosen randomly, and two different distances were measured by two observers. The measurements were made twice at an interval of at least 2 weeks.

RESULTS

Anatomical layers and boundaries of the temporal area

After the dissection, the superficial temporal fascia (STF), innominate fascia (IF), DTF, superior temporal septum (STS), inferior temporal septum (ITS), and temporal ligamentous adhesion (TLA) were observed (Fig. 2, Supplemental Video 1).

The anatomical layers of the temporal area were identified as the skin (layer 1), subcutaneous fat tissue (layer 2), STF (layer 3), IF (layer 4), and DTF (layer 5). The most superficial layer

Fig. 1. Illustrations of craniometric landmarks and semi-landmarks

Lateral (A) and basal (B) views of the skull. The landmarks (red dots) and semi-landmarks (blue dots) are described in Table 1.

Fig. 2. Schematic of boundaries of the temporal area

HB, harvestable boundary of the deep temporal fascia (blue broken line); ITS, inferior temporal septum; LOT, lateral orbital thickening; LTC, lower temporal compartment (green shaded area); STFP, superficial temporal fat pad; STS, superior temporal septum; SV, sentinel vein; TFN, temporal branch of the facial nerve; TLA, temporal ligamentous adhesion; UTC, upper temporal compartment (purple shaded area); ZTN, zygomaticotemporal nerve.
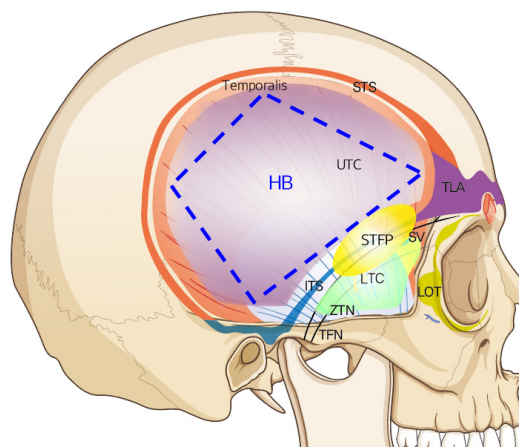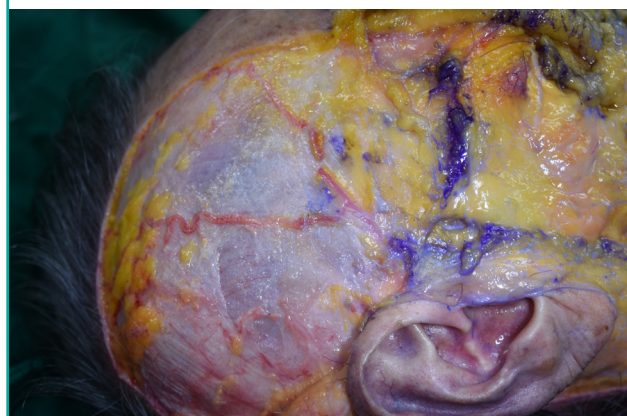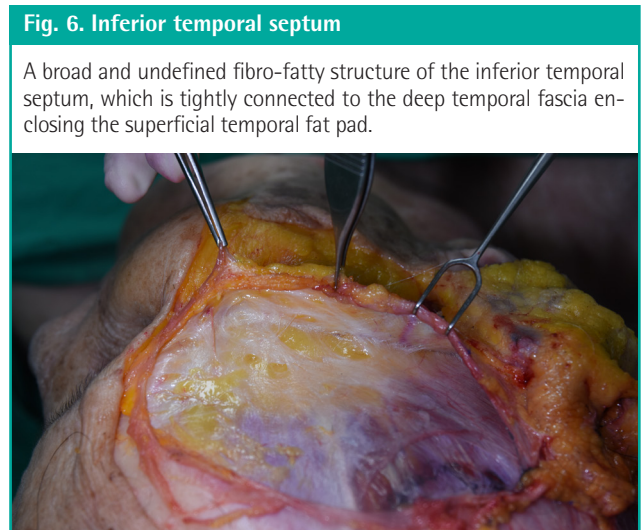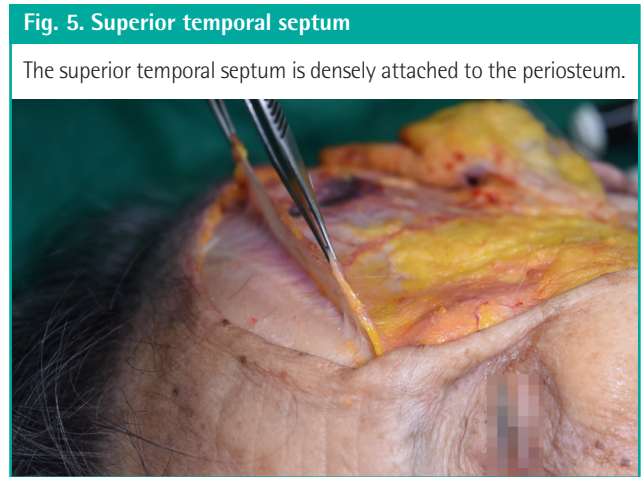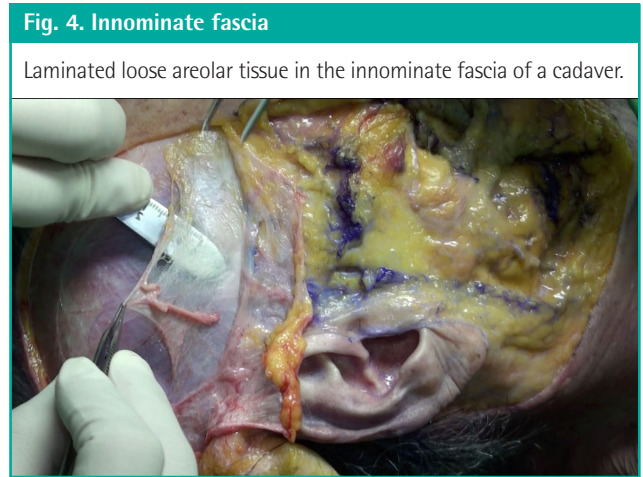

Fig. 3. Superficial temporal fascia

The superficial temporal artery and vein are visible in the superficial temporal fascia.

was the STF. The superficial temporal artery and vein ran through the STF and divided into the anterior and posterior branches 3 cm above the zygomatic arch (Fig. 3). The IF was a laminated loose areolar layer between the STF and the DTF

Fig. 4. Innominate fascia

Laminated loose areolar tissue in the innominate fascia of a cadaver.

Fig. 5. Superior temporal septum

The superior temporal septum is densely attached to the periosteum.

Fig. 6. Inferior temporal septum

A broad and undefined fibro-fatty structure of the inferior temporal septum, which is tightly connected to the deep temporal fascia enclosing the superficial temporal fat pad.

(Fig. 4). The STS was densely attached to the periosteum superoposteriorly and continued to the DTF (Fig. 5). The ITS was a broad and undefined fibro-fatty structure tightly connected with the DTF (Fig. 6). The superior and inferior temporal septa merged anteriorly into the TLA. The DTF was composed of superficial and deep laminae. The superficial temporal fat pad was enclosed between these two laminae under the ITS (Fig. 7).

The boundary of the ETC was the STS superoposteriorly, the TLA anteriorly, the upper border of the zygomatic arch anteroinferiorly, the IF laterally, and the DTF medially. The UTC and the LTC were divided by the ITS and the TLA. The UTC was easily dissected, and no major neurovascular structures were observed (Fig. 8). The boundary of the UTC was the STS superoposteriorly, the ITS anteroinferiorly, and the level of the upper border of the zygomatic arch posteroinferiorly. The LTC is anatomically complex due to its fibro-fatty components and neurovascular structures.

Fig. 7. Superficial temporal fat pad

The superficial temporal fat pad is located between the superficial and deep laminae of the deep temporal fascia.

Fig. 8. Upper temporal compartment

The upper temporal compartment is located between the superior temporal septum and the inferior temporal septum and contains no major neurovascular structures.

Chi D et al.   Deep temporal fascia in Asian cadavers
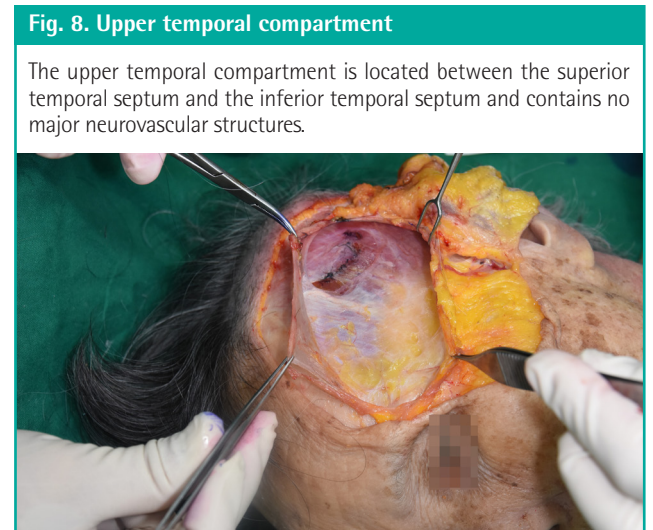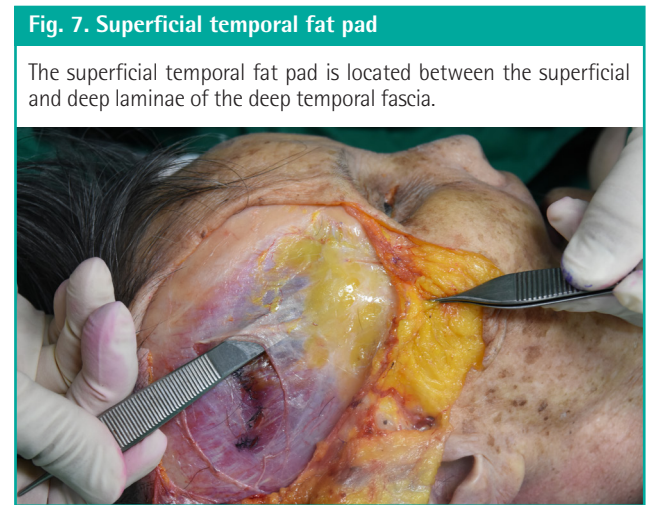
Archives of Plastic Surgery APS

Fig. 9. Landmarks and semi-landmarks

Landmarks and the semi-landmarks were placed on the image to enable the calculation of the deep temporal fascia's dimensions.
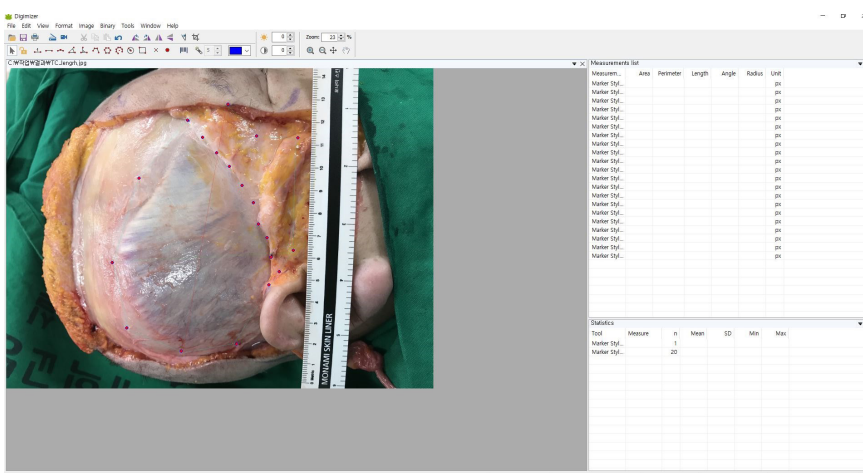

Fig. 10. Temporal compartment lengths

(A) Vertical (blue line) and horizontal (red line) lengths of the entire temporal compartment (blue shaded area). (B) Vertical (blue line) and horizontal (red line) lengths of the upper temporal compartment (yellow shaded area).
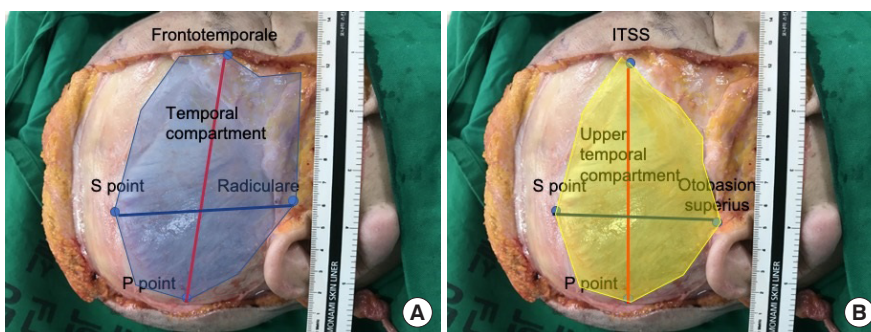

Table 2. Intraobserver and interobserver reliability assessment

Evaluation	Intraobserver, ICC (95% CI)		Interbserver, ICC (95% CI)	
	Observer 1	Observer 2	Session 1	Session 2
Evaluation 1	0.993 (0.971–0.998)	0.983 (0.933–0.996)	0.975 (0.905–0.994)	0.971 (0.890–0.993)
Evaluation 2	0.982 (0.931–0.996)	0.989 (0.955–0.997)	0.948 (0.807–0.987)	0.943 (0.790–0.986)

ICC, interclass correlation coefficient; CI, confidence interval.

Measurement of temporal compartment dimensions

The intraobserver and interobserver agreement showed high consistency (interclass correlation coefficient > 0.75) (Table 2). The five landmarks of the temporal fossa were placed on the digital images, and 15 semi-landmarks were added to represent the detailed curvature of the temporal compartments (Fig. 9). Eight of the 20 landmarks and semi-landmarks were used to measure the vertical and horizontal lengths of the temporal compartments (Fig. 10). The vertical and horizontal lengths of the ETC were 7.74 ± 0.53 cm and 11.36 ± 0.72 cm, respectively. The vertical and horizontal lengths of the UTC were 6.41 ± 0.67 cm and 10.44 ± 0.83 cm, respectively (Table 3). To measure the surface area of the temporal compartments, the set of points

Table 3. Overall length of the temporal compartments

Variable	Distance (cm)	
	Mean ± SD	Median (range)
TCVL	7.74 ± 0.53	7.82 (6.60–8.80)
TCHL	11.36 ± 0.72	11.01 (10.17–13.15)
UTCVL	6.41 ± 0.67	6.40 (5.27–7.50)
UTCHL	10.44 ± 0.83	10.26 (9.2–11.70)

TCVL, vertical length of the entire temporal compartment; TCHL, horizontal length of the entire temporal compartment; UTCVL, vertical length of the upper temporal compartment; UTCHL, horizontal length of the upper temporal compartment.

with landmarks and semi-landmarks was linked together on the images (Fig. 11). The average surface area of the ETC, UTC,
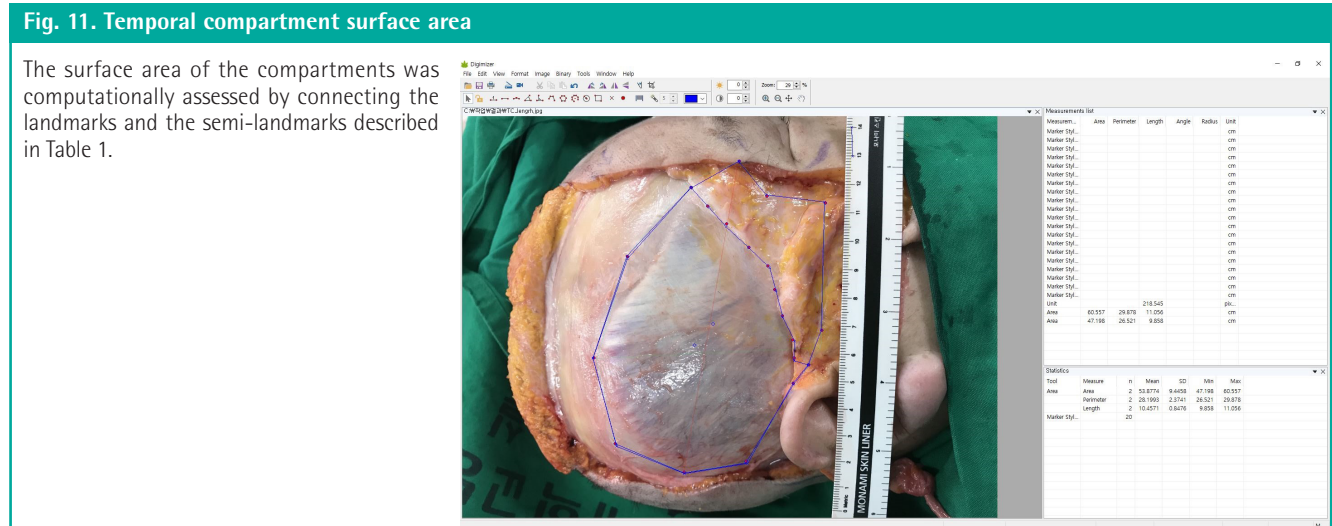
Fig. 11. Temporal compartment surface area

The surface area of the compartments was computationally assessed by connecting the landmarks and the semi-landmarks described in Table 1.

Table 4. Overall surface area of the temporal compartments

| Variable | Area (cm²) | |
	Mean ± SD	Median (range)
ETC	63.78 ± 6.04	64.72 (52.43–73.42)
UTC	48.52 ± 5.65	48.16 (40.03–61.56)
LTC	15.26 ± 3.97	15.02 (9.21–23.96)

ETC, entire temporal compartment; UTC, upper temporal compartment; LTC, lower temporal compartment.

Table 5. Sex differences in the length of the temporal compartments

| Variable | Distance (cm) | | t | P-value[a] |
	Male	Female		
TCVL	7.57 ± 0.60	7.86 ± 0.45	0.77	0.449
TCHL	11.49 ± 0.89	11.27 ± 0.59	−1.456	0.158
UTCVL	6.42 ± 0.59	6.40 ± 0.73	−0.168	0.868
UTCHL	10.40 ± 0.92	10.46 ± 0.79	0.058	0.954

Values are presented as mean ± SD.
TCVL, vertical length of the entire temporal compartment; TCHL, horizontal length of the entire temporal compartment; UTCVL, vertical length of the upper temporal compartment; UTCHL, horizontal length of the upper temporal compartment.
[a]Statistically significant, P < 0.05.

Table 6. Sex differences in the surface area of the temporal compartments

| Variable | Area (cm²) | | t | P-value[a] |
	Male	Female		
ETC	64.45 ± 5.27	63.31 ± 6.64	0.474	0.639
UTC	48.10 ± 5.32	48.80 ± 6.02	−0.311	0.758
LTC	16.35 ± 3.57	14.51 ± 4.17	1.192	0.244

Values are presented as mean ± SD.
ETC, entire temporal compartment; UTC, upper temporal compartment; LTC, lower temporal compartment.
[a]Statistically significant, P < 0.05.

and LTC were 63.78 ± 6.04 cm², 48.52 ± 5.65 cm², and 15.26 ± 3.97 cm², respectively (Table 4). Although there were some differences in the results between the sexes, they were not statistically significant (P > 0.05) (Tables 5, 6).

DISCUSSION

Harvesting the DTF without a sufficient anatomical understanding often causes postoperative complications such as bleeding, facial nerve paralysis, and temporal hollowness [15-

19]. Previous studies reported the LTC contained all of the "at-risk" anatomical structures of the temporal area [12,15,20]. Moss et al. [12] reported that the sentinel vessels and both branches of the zygomaticotemporal nerve cross the LTC from deep to superficial on the inferomedial surface of the ITS. Huang et al. [20] reported that the anterior half of the LTC, where the sentinel vein and branches of the middle temporal vessels perforate the temporal fascia and travel into the subcutaneous tissue layer, is a "zone of caution." Vaca et al. [15] reported that preserving the superficial temporal fat pad on the ITS prevented postoperative temporal hollowness. We agree with the findings of those studies because of the anatomical complexity of the LTC.

In contrast, the layers and the ligamentous structures of the UTC were readily identified, as described in previous studies [11,12]. These structures are important for defining the boundary of the UTC and provide vital information about safe dissection. No major neurovascular structures were identified in the UTC. Therefore, the UTC is a surgically safe space through which one can easily harvest the DTF in rhinoplasty.

Several studies have reported harvestable boundaries of the

Chi D et al.   Deep temporal fascia in Asian cadavers

Archives of Plastic Surgery APS

Fig. 12. Deep temporal fascia contraction after harvest

Maximum harvestable boundary of the deep temporal fascia of a cadaver before (approximately 7 × 10 cm) (A) versus immediately after (approximately 5 × 8 cm) (B) harvest.
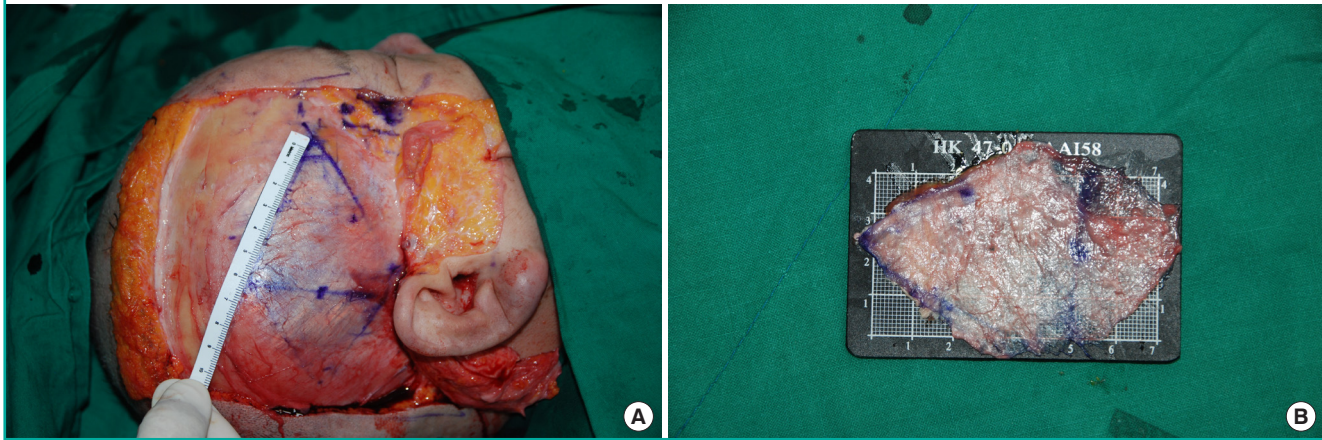
DTF and its maximum dimensions; however, its safe boundaries have not been described in detail [21-24]. Moran reported that each margin of the DTF ended in periosteal attachments at the frontal and parietal bones and at the upper edge of the zygomatic arch and that the maximum dimensions of the DTF were within 7 × 7 cm [21]. Daniel and Palhazi [22] harvested the DTF with the resection superiorly to the periosteal junction, anteriorly to the DTF split, inferiorly toward the concha, and posteriorly as far back as possible. They usually harvested a 5 × 5 cm or larger piece of the DTF. Despite significant variations among individuals, Miller reported that a DTF sheet measuring approximately 4 × 6 cm could be obtained with a thickness of approximately 1 mm [23]. Considering the risk of dissecting the ITC, the maximum harvestable boundary of the DTF is similar to that of the UTC, which had a mean value of 6.41 × 10.44 cm in this study.

Rohrich et al. [24] incised the temporal fascia close to the attachments of the temporalis muscle to the skull periosteum superiorly and posteriorly and where it began to divide into the deep and superficial layers anteriorly and harvested the temporal fascia inferior to the level of the ear. They reported that the temporal fascia was approximately 8 × 6 cm; however, it contracted to approximately 5 × 4 cm after the harvest. In addition, human and animal studies reported that the DTF contracts by 15%–40% after harvest [25,26]. We also identified that the DTF measured 7 × 10 cm before harvest and contracted to 5 × 8 cm immediately after harvest (Fig. 12). Thus, a larger DTF area than needed should be harvested to compensate for the contraction.

Morphological differences in skulls between races and sex were reported previously [27]. It is generally accepted that dolichocephalic Caucasians have larger harvestable DTF areas than brachycephalic Asians owing to their anteroposteriorly long skull diameter. However, only a few studies have investigated the dimensions of the DTF, and most were conducted in Caucasians [21-24]. Moreover, no studies have compared the dimensions of the temporal area among different races. Prior to this study, we assumed that males had larger DTF areas than females considering the differences in their head sizes. However, we did not find statistically significant sex-based differences in any dimensions.

This study has some limitations. First, its sample size was small, and all samples were Korean. To reduce statistical errors and evaluate the differences among variable groups including race, sex, age, and height, sample size and diversity must be increased in further studies. Second, three-dimensional structures were measured by two-dimensional photogrammetric analysis, which always causes measurement errors regardless of intensity. Although two observers performed the measurements and the reliability assessment to avoid errors, this approach may not be sufficiently quantitative to ensure analytic precision.

In conclusion, use of the UTC enables sufficient DTF harvesting for clinical applications in rhinoplasty. A thorough understanding of the UTC boundary enables the easy and safe harvest of a sufficient amount of DTF.

NOTES

Conflict of interest

No potential conflict of interest relevant to this article was reported.

Ethical approval

The study was approved by the Institutional Review Board of Chungnam National University Hospital (IRB No. 2019-03-

042) and performed in accordance with the principles of the Declaration of Helsinki.

Patient consent

The cadavers' guardian provided written informed consent for the publication and the use of images.

Author contribution

Conceptualization: D Chi, TK Kim. Data curation: S Kim. Formal analysis: JH Kim. Funding acquisition: SH Oh. Methodology: JH Kim. Project administration: JY Jeong, SH Oh. Visualization: C Shin. Writing - original draft: D Chi. Writing - review & editing: S Kim, SH Oh.

ORCID

Daekwan Chi   https://orcid.org/0000-0003-3903-4008
Jae-Hee Kim   https://orcid.org/0000-0001-8022-4896
Taek-Kyun Kim   https://orcid.org/0000-0002-3213-9803
Jae Yong Jeong   https://orcid.org/0000-0001-5654-4443
Chungmin Shin   https://orcid.org/0000-0002-0613-649X
Sunje Kim   https://orcid.org/0000-0001-7887-7521
Sang-Ha Oh   https://orcid.org/0000-0003-3734-5005

Supplementary material

Supplemental Video 1. Temporal area dissection. Supplemental data can be found at: https://doi.org/10.5999/aps.2020.01165.v001.

REFERENCES

1. Nakajima H, Imanishi N, Minabe T. The arterial anatomy of the temporal region and the vascular basis of various temporal flaps. Br J Plast Surg 1995;48:439-50.
2. Han KH, Yeo HJ, Choi TH, et al. Rhinoplasty using various autogenous tissues. J Korean Soc Plast Reconstr Surg 2010;37:37-45.
3. Jeong JY. Rebuilding nose: rhinoplasty for Asians. Uijeongbu: Medic Medicine; 2018.
4. Suh MK. Dorsal augmentation using autogenous tissue. In: Suh MK, Harijan A, Kim ST, editors. Atlas of Asian rhinoplasty. Singapore: Springer; 2018. p. 171-208.
5. Park SW, Kim JH, Choi CY, et al. Various applications of deep temporal fascia in rhinoplasty. Yonsei Med J 2015;56:167-74.
6. Kim HK, Rhee SC. Augmentation rhinoplasty using a folded "pure" dermal graft. J Craniofac Surg 2013;24:1758-62.
7. Karaaltin MV, Batioglu-Karaaltin A, Orhan KS, et al. Autologous fascia lata graft for contour restoration and camouflage

8. in tertiary rhinoplasty. J Craniofac Surg 2012;23:719-23.
9. Hong ST, Kim DW, Yoon ES, et al. Superficial mastoid fascia as an accessible donor for various augmentations in Asian rhinoplasty. J Plast Reconstr Aesthet Surg 2012;65:1035-40.
10. Guerrerosantos J. Temporoparietal free fascia grafts in rhinoplasty. Plast Reconstr Surg 1984;74:465-75.
11. Han JW, Sun H. Refinement of intraoral reverse temporalis transfer for facial palsy using a mandibular periosteum flap. Arch Plast Surg 2020;47:198-9.
12. O'Brien JX, Ashton MW, Rozen WM, et al. New perspectives on the surgical anatomy and nomenclature of the temporal region: literature review and dissection study. Plast Reconstr Surg 2013;131:510-22.
13. Moss CJ, Mendelson BC, Taylor GI. Surgical anatomy of the ligamentous attachments in the temple and periorbital regions. Plast Reconstr Surg 2000;105:1475-90.
14. Noback ML, Harvati K. Covariation in the human masticatory apparatus. Anat Rec (Hoboken) 2015;298:64-84.
15. Toro-Ibacache V, Zapata MuNoz V, O'higgins P. The predictability from skull morphology of temporalis and masseter muscle cross-sectional areas in humans. Anat Rec (Hoboken) 2015;298:1261-70.
16. Vaca EE, Purnell CA, Gosain AK, et al. Postoperative temporal hollowing: Is there a surgical approach that prevents this complication? A systematic review and anatomic illustration. J Plast Reconstr Aesthet Surg 2017;70:401-15.
17. Kim S, Matic DB. The anatomy of temporal hollowing: the superficial temporal fat pad. J Craniofac Surg 2005;16:760-3.
18. Park JA, Lee SH, Ha TJ, et al. Location of the split line of the deep temporal fascia when reducing a zygomatic arch fracture. J Plast Reconstr Aesthet Surg 2020;73:1130-4.
19. Lee JS, Kim JS, Lee JW, et al. Correction of microtia with constriction features using a superficial temporal fascial flap combined with a rib cartilage graft. Arch Plast Surg 2020;47:317-23.
20. Cheon JH, Lee HC, Im GJ, et al. Safety and efficacy of transcutaneous bone conduction implant surgery for hearing improvement in microtia patients with bilateral hearing impairment. Arch Plast Surg 2019;46:525-34.
21. Huang RL, Xie Y, Wang W, et al. Anatomical study of temporal fat compartments and its clinical application for temporal fat grafting. Aesthet Surg J 2017;37:855-62.
22. Moran SL. Temporoparietal fascia flap. In: Wei FC, Mardini S, editors. Flaps and reconstructive surgery. Philadelphia: Elsevier; 2009. p. 159-73.
23. Daniel RK, Palhazi P. Rhinoplasty: an anatomical and clinical atlas. New York: Springer; 2018.
24. Miller TA. Temporalis fascia grafts for facial and nasal con-

Chi D et al. Deep temporal fascia in Asian cadavers

Archives of Plastic Surgery APS

tour augmentation. Plast Reconstr Surg 1988;81:524-33.

24. Rohrich RJ, Adams WP, Ahmad J, et al. Dallas rhinoplasty: nasal surgery by the masters. Boca Raton: CRC Press; 2014.

25. Indorewala S. Dimensional stability of the free fascia grafts: an animal experiment. Laryngoscope 2002;112:727-30.

26. Indorewala S, Pagare R, Aboojiwala S, et al. Dimensional stability of the free fascia grafts: a human study. Laryngoscope 2004;114:543-7.

27. Jamieson A, Moenssens AA. Wiley encyclopedia of forensic science. New Jersey: Wiley; 2009.